Effect of various initial concentrations of CTAB on the noncovalent modified graphene oxide (MGNO) structure and thermal stability

Ferda Mindivan, Bilecik, Turkey

Article Information

Correspondence Address
Assistant Prof. Dr. Ferda Mindivan
Department of Technical Programs
Bozuyuk Vocational College
Bilecik S.E. University
Bilecik, 11210, Turkey.
E-mail: ferda.mindivan@bilecik.edu.tr

Keywords
GO, CTAB, non-covalent modification, intercalation, thermal stability

Graphene oxide (GO) was prepared by oxidation reaction of graphite (GF) using the Hummers' method and modified by a cationic surfactant (cetyltrimethylammonium bromide – CTAB) followed by chemical reduction using hydrazine monohydrate ($N_2H_4 \times H_2O$) to obtain MGNO powders. The structural and thermal properties of GO and MGNO powders were studied using zeta potentiometer (ZP), Fourier transform infrared spectroscopy (FTIR), X-ray diffraction (XRD), scanning electron microscopy (SEM) and thermogravimetric analysis (TGA). The results demonstrated that CTAB was successfully grafted onto the surface of the GO through non-covalent modification between CTA^+ ions and GO for all MGNO powders. A reasonable improvement in thermal stability of the MGNO powders was also observed. FTIR results showed the successful intercalation of CTA^+ ions for all MGNO powders. The optimum concentration of surfactant was found to be 120 mg × l^{-1} (MGNO-120) by using analysis results. The ease of synthesis of MGNO-120 with both excellent intercalation and thermal stability will greatly facilitate potential applications.

Organic or inorganic fillers such as silicates, clay, carbon fibers and carbon nanotubes have been extensively studied in both academic and commercial communities over the past decades [1, 2]. In the recent trend, graphene derivatives such as graphene oxide (GO), reduced graphene oxide (RGO) and modified graphene oxide (MGNO) have received attention as fillers in composites [3]. The dispersion of the fillers within the polymer matrix is important to form intercalated or exfoliated composites and to improve the thermal and mechanical properties of the composites [4]. Pristine graphene is hydrophobic, tends to agglomerate irreversibly [5], does not disperse well in polymers and has a tendency to form phase separated composites [6].

GO has attracted interest because of its easy synthesis, solution processability, large surface area and layered structure [3, 7, 8]. Usually, GO is prepared from oxidation of graphite (GF) by Hummers' method. GO containing hydroxyl and epoxide groups on the basal plane and carboxylic acid groups at the edges (see Figure 1) are hydrophilic and capable of forming stable colloidal suspensions [4, 9]. Additionally, functionalized or modified GO synthesized by chemical modification of graphene using surfactants are used to provide better interactions with the host polymers compared to pristine graphene or GF [10, 11]. The surface modification of graphene can be performed by chemical bonds (covalent modification) or π-π interactions (noncovalent modification) and followed by reduction [6]. Noncovalent modification is generally preferred because it does not destroy the intrinsic structure of graphene and preserves its excellent properties [12].

In this study, cetyltrimethylammonium bromide (CTAB), a type of cationic surfactant, is used to modify GO via noncovalent modification and this molecule consists of a cationic ammonium head group and a

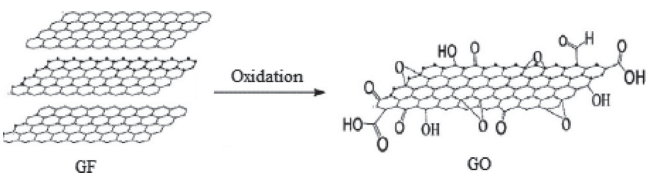

Figure 1: The schematic diagram of the oxidation reaction of GF [17]

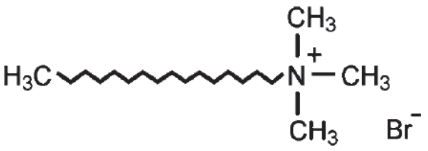

Figure 2: Structure of a CTAB molecule [18]

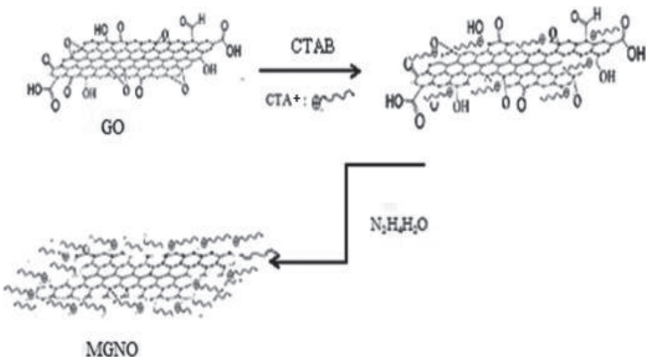

Figure 3: The schematic diagram of the preparation of MGNO from GO

long alkyl chain as tail (see Figure 2) [13]. The negatively charged carboxyl group of GO can interact with the positive charged CTA^+ through ionic interactions, and then, the CTAB-GO is reduced by hydrazine monohydrate ($N_2H_4 \times H_2O$) to form MGNO (see Figure 3) [5, 14]. In previously papers, only one concentration of surfactants for modification and prepared powders was used as a filler to fabricate polymer matrix composites [10, 14-16]. However, there are no published data concerning the effect of the various initial concentrations of CTAB on the structural and thermal characteristics of MGNO. The aim of this work is to investigate the interactions between GO sheets and CTA^+ ions in aqueous dispersions and the structural and thermal characteristics of MGNO by using ZP, FTIR, XRD, SEM and TGA as a function of various initial concentrations of CTAB, and prepared MGNO powders can be used as a filler to fabricate high-performance graphene-based polymer composites or nanocomposites.

Experimental details

Materials. GF powder (45 μm nominal particle size), CTAB and $N_2H_4 \times H_2O$ were of reagent grade and purchased from Merck. All these agents were used without further purification.

Preparation of modified graphene oxide (MGNO). GO was synthesized using the modified Hummers' method [19] and the details of the process were given previously [20]. GO was modified using CTAB in ultrasonic bath as follows: GO (0.1 g) was dispersed in 100 ml distilled water with various initial concentrations of CTAB (30, 120, 200, 300 mg × l^{-1}) under ultrasonic agitation, then 2 ml $N_2H_4 \times H_2O$ was added into the mixture. Then, the mixture was heated to 95 °C for 12 h. After that, the mixture was centrifuged to remove excess hydrazine and CTAB. By changing the various initial concentrations of CTAB in the resulting powders, a series of MGNO powders was prepared and coded as MGNO-30, MGNO-120, MGNO-200 and MGNO-300.

Characterization. Surface charges of powders dispersed in water using ultrasonication were measured by Zetasizer (Malvern Instruments Ltd., UK). Structural analyses of

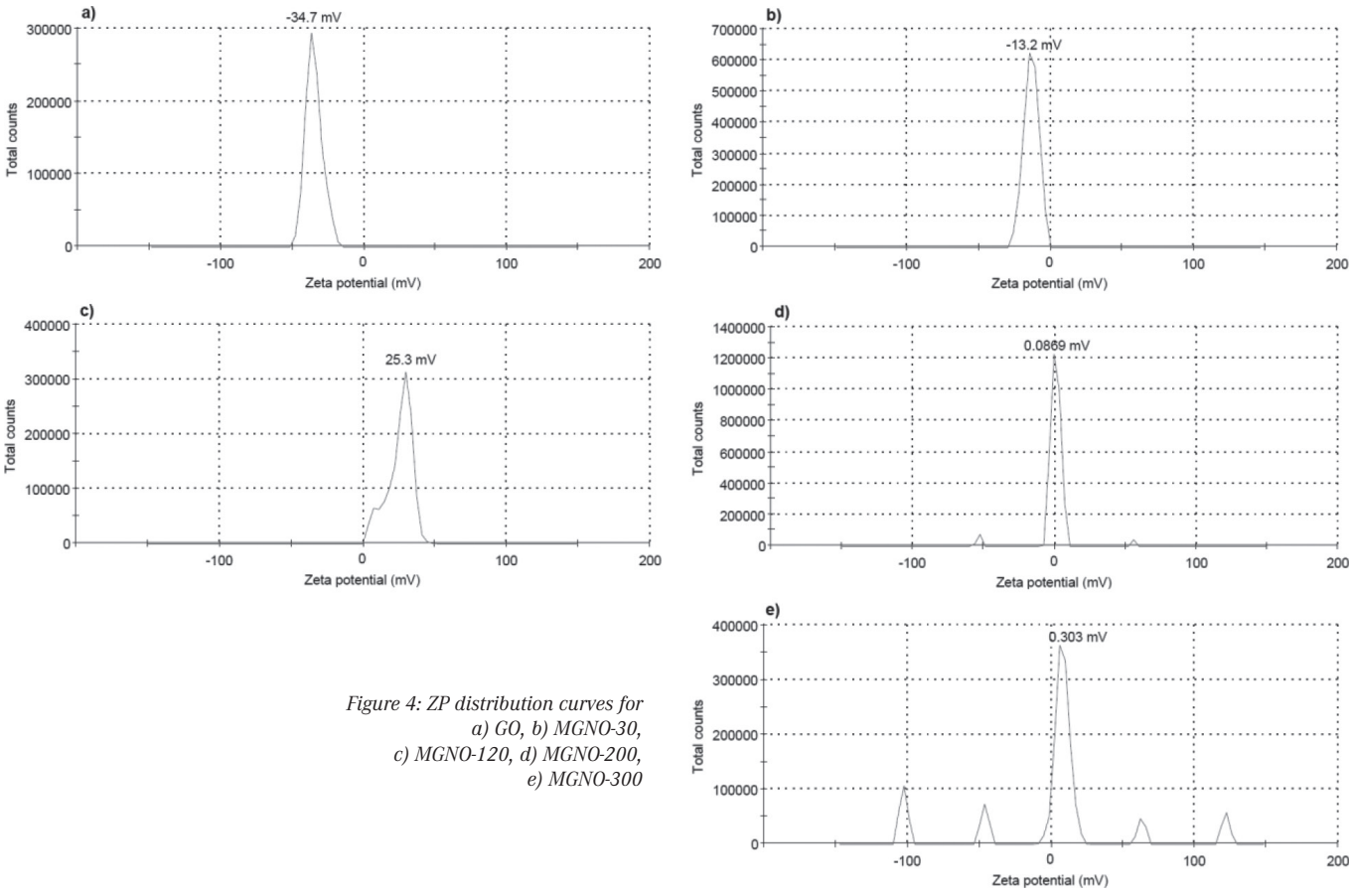

Figure 4: ZP distribution curves for a) GO, b) MGNO-30, c) MGNO-120, d) MGNO-200, e) MGNO-300

the samples were carried out by FTIR spectra (Spectrum 100, Perkin Elmer) in the range of 4000-400 cm^{-1} and X-ray diffraction (XRD, PAN analytical, Empyrean) in the range of $2\theta = 5\text{-}40°$ using Cu K_α radiation ($\lambda = 0.15405$ nm). The surface morphology was examined by a scanning electron microscopy (SEM, Supra 40VP, Zeiss) coupled with energy dispersive spectrometer (EDS). Thermogravimetric analysis (TGA, STA 409, Netzsch) was performed by heating the samples from 25 °C to 600 °C at a rate of 20 °C × min^{-1} in nitrogen atmosphere.

Results and discussion

Zeta potentials (ZP) measurements. The change of the surface charge of the GO due to the CTAB treatment was confirmed by ZP measurements. The zeta potential distribution and surface charge values of GO and MGNO dispersions are shown in the Figures 4a to 4e and the orientation and stacking mechanisms which predominate at various initial concentrations of CTAB have been schematically shown in the Figures 5a to 5d.

The ZP value of GO was found to be -34.7 mV. The negative ZP values were due to the presence of oxygen containing functional groups formed at the graphite lattice during the oxidation (see Figures 1 and 4a) [21]. Net ZP increased with modification of GO by various initial concentrations of CTAB. As shown in Figure 4b, the ZP value for MGNO-30 was -13.2 mV. This value can be compared to the ZP of GO (-34.7 mV). The lower negative ZP of the MGNO-30 was due to a decrease in oxygen containing functional groups by reduction. However, the negative sign of the surface charge did not change in the 30 mg × l^{-1} concentration of CTAB because the number of CTA^+ ions was not enough to change the surface charge sign (see Figure 5a). When the concentration of CTAB increased to 120 mg × l^{-1}, the ZP value was +25.3 mV (see Figure 4c). This significant shift of ZP would be an evidence for the best modification of CTA^+ ions on the GO surface. So, the positively charged CTA^+ ions are attached with the negatively charged $^-$OH and $^-$COOH groups of GO through the electrostatic interactions, resulting in stable sheets with CTA^+ immobilized on the edge or surface of GO sheets (see Figure 5b). Both MGNO-200 and MGNO-300 exhibited net positive ZP values with the distribution peaks centered at 0.0869 and 0.303 mV, respectively (see Figures 4d and 4e). At the same time, multiple peaks were observed in the same ZP curves because CTA^+ ions aggregated at high CTAB concentrations (200 mg × l^{-1} and 300 mg × l^{-1}) (see Figures 5c and 5d). For electrostatic reasons, colloidal particles with a ZP value less than -15 mV or more than 15 mV are expected to be stable [22, 23]. In this case, MGNO-30 and MGNO-120 had higher stability than MGNO-200 and MGNO-300.

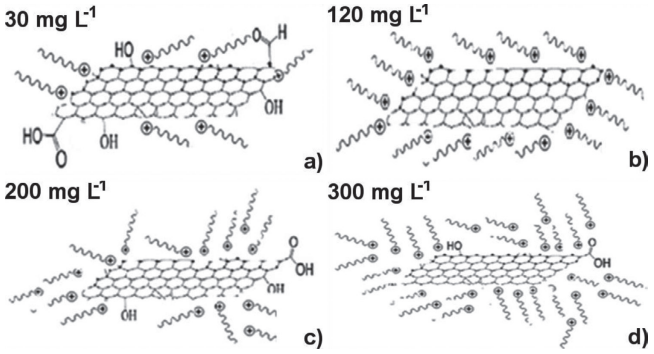

Figure 5: Schematic illustration of the orientation and stacking of CTA^+ ions on surface of a) MGNO-30, b) MGNO-120, c) MGNO-200, d) MGNO-300

FTIR analysis. Figure 6 shows the FTIR spectrum of GO powder and MGNO powders synthesized with various initial concentrations of CTAB. Characteristic peaks were observed for GO: the broad peak at 3000-3500 cm^{-1} could be assigned to the O–H stretching vibrations of carboxylic, carbonyl, epoxy and hydroxyl groups in GO [11]. Two peaks located at 1768 cm^{-1} and 1652 cm^{-1} belong to the C = O (carbonyl and carboxyl) and the C = C skeletal stretching vibrations, respectively [24]. In addition, the characteristic C-O (epoxy) and C-O (alkoxy) stretching vibration bands could be observed at 1213 cm^{-1} and 1000 cm^{-1}, respectively. These results suggested that the GO sample was fully oxidized [25] as given in Figure 6. FTIR spectrum of MGNO powders showed that the bands of GO at 3342 cm^{-1} of O-H and 1768 cm^{-1} of carboxyl disappeared and also the intensity of bands at 1213 cm^{-1} and 1000 cm^{-1} decreased. These results showed that functional groups containing oxygen were removed by hydrazine [26]. The bands at 1555 cm^{-1} were assigned to N-H bending vibration which showed the coexistence of the amide bond generated with amino groups in the CTAB, and carboxy groups in the GO in all MGNO powders [14]. The bands at 2926 cm^{-1} and 2855 cm^{-1} in curves of all MGNO powders were ascribed to C-H stretching vibrations of the alkyl chain of CTAB [15]. These peaks seemed more severe at the FTIR spectrum of MGNO-120. The band at 1039 cm^{-1} (C-O-C stretching vibrations) for the MGNO-120 indicated the interaction between CTAB and the epoxy group of GO [27]. The FTIR

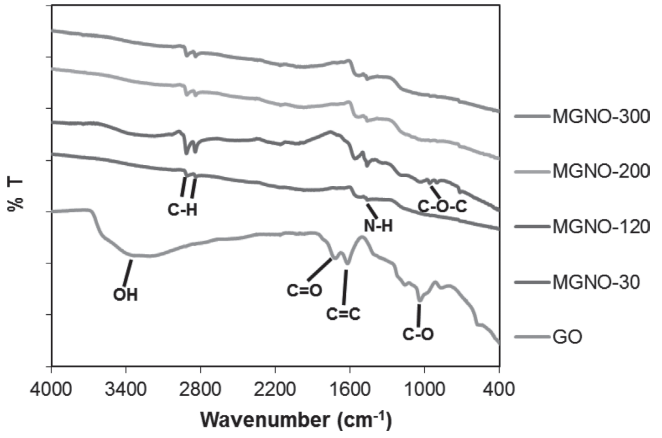

Figure 6: FTIR spectrum of GO and MGNO powders

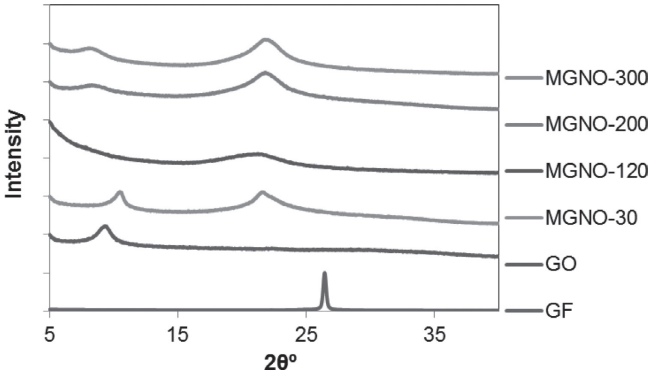

Figure 7: XRD patterns of GF, GO and MGNO powders

results showed the successful intercalation of CTA^+ ions for all MGNO powders, but the best intercalation was observed for the MGNO-120 powder.

XRD analysis. The XRD patterns of GF, GO and MGNO powders are shown in Figure 7. The crystalline GF powder presented a typical diffraction peak at $2\theta = 26.4°$. The corresponding interlayer distance was observed to be 0.33 nm. After oxidation, the diffraction peak of GO appeared at about $2\theta = 9.9°$, indicating that the interlayer space increased to 0.88 nm. The increase in the interlayer distance from 0.33 nm to 0.88 nm was due to oxygen containing functional groups intercalated within the layered structure [3, 11, 28]. From the XRD pattern of powders (see Figure 7), a small diffraction peak at $2\theta = 10.6°$ appeared in the MGNO-30 powder, and both the MGNO-200 and MGNO-300 powders showed a broad diffraction peak at $2\theta = 8.5°$ which indicated the coexistence of CTAB and GO in the MGNO powders [14]. This is supported by the results of FTIR (see Figure 6). Meanwhile, a small diffraction peak in MGNO-30, MGNO-200 and MGNO-300 was observed at $2\theta = 21.8°$. This confirmed the reduction process from GO to MGNO by hydrazine monohydrate [26]. In the XRD pattern of MGNO-120 (see Figure 7), there was a weak and wide diffraction peak located at $2\theta = 21.1°$, indicating that the graphene sheets were intercalated totally after the modification. No other diffraction peaks were observed except the weak diffraction peak of MGNO-120. This meant that GO layers were completely separated [29]. Wu et al. [14] reported that CTAB made the GO layers thinner.

SEM analysis. Figures 8a to 8f show the SEM images of the GF and prepared GO and MGNO powders. It could be clearly seen from the SEM image of Figure 8a that GF had a thin plate stacked structure [30]. The aggregated and randomly accumulated sheets for GO with a worm-like structure were observed, which were consistent with previous studies (see Figure 8b) [31, 32]. According to EDS results of the GF and GO, GF exhibited oxygen content of 22.59 at.-%. After oxidation, GO had oxygen content of 47.95 at.-%, which indicated full oxidation. From Figure 8c, it could be seen that the MGNO-30 powder exhibited a smooth layered structure showing the effect of low concentration of CTAB. As shown in the Figures 8d to 8f, the SEM images of the MGNO-120, MGNO-200 and MGNO-300 powders exhibited wrinkle, layered and dense stacked structure due to reduction and modification reactions [15, 16]. From Figure 8d, it could be observed that, when the content of CTAB was 120 mg × l^{-1}, GO layers were separated from each other which was also supported by the XRD pattern of MGNO-120 (see Figure 7).

TGA analysis. The TGA and derivative thermograms (DTG) curves of GO and MGNO powders are shown in Figures 9a to 9e. Peak temperature (T_p), weight loss (%) and residue amounts (%) obtained from TGA and DTG curves are summarized in Table 1.

As shown in Figure 9a, the first weight loss was observed in 78 °C for the GO, corresponding to the loss of water molecules [33]. GO showed a major weight loss at the DTG peak at 185 °C (see Table 1) assigned to the removal of most of the oxygen containing functional groups [34]. A small weight loss at 269 °C from pyrolysis of the unstable oxygen functionalities was attributed to CO, CO_2 and steam release [16]. The last step at 558 °C was related to pyrolysis of the remaining oxygen-containing groups as well as the burning of ring carbon [35] (see Figure 9a and Table 1). GO exhibited about 13 % residual weight at 600 °C.

The MGNO powders showed a medium weight loss at the temperature range of 53-66 °C, clearly due to evaporation of water molecules. As shown in Figures 9b to 9e and Table 1, the main step of degradation appeared at 209 °C and 232 °C (T_{P2}) for the MGNO powders. This main step of thermal degradation was the decomposition of CTAB in the interlayer of GO [14] and the last decomposition occurred in the range of 288-351 °C (T_{P3}), which correspond to the loss of remaining oxygen functionalities of MGNO [6]. All the MGNO powders exhibited higher T_{P2} and T_{P3} temperatures than GO, indicating that the presence of CTAB could increase thermal stability. Such high thermal stability of the MGNO powders could be attributed to the very strong interactions between CTA^+ ions and GO [36]. When the temperature reached 600 °C, the weight losses for MGN0-30, MGNO-120, MGNO-200 and MGNO-300 powders were almost 31.7, 60.7, 61.0 and 46.6 %, respectively. These values were less than the 86.7 % loss at 600 °C for GO (see Table 1). These results showed that MGNO powders had much higher thermal stability than GO because of successful intercalation between CTA^+ ions with GO.

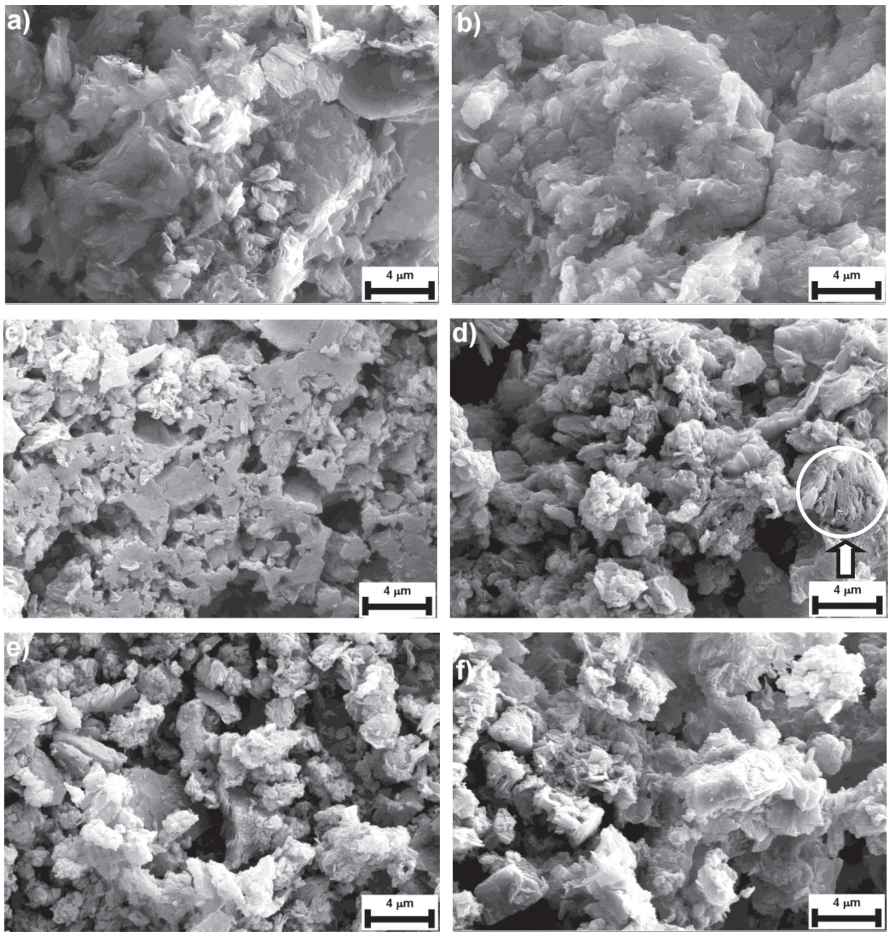

Figure 8: SEM images (magnification 10.000×) of a) GF, b) GO, c) MGNO-30, d) MGNO-120, e) MGN0-200, f) MGNO-300

Conclusions

The main findings of the study can be summarized as follows:

- All analysis results showed that GO was successfully synthesized from natural graphite by Hummers' method.
- The high negative ZP of GO was due to the oxygen containing functional groups. After the CTAB treatment, the negative sign of the surface charge did not change in the MGNO-30, but the MGNO-120 with the highest positive ZP value (25.3 mV) which demonstrated the highest stability.
- The FTIR results showed the successful intercalation of CTA^+ ions for all MGNO powders, but the best intercalation was obtained for the MGNO-120 powder.
- For all MGNO powders, the interlayer distance of GO sheets was increased by the CTAB modification, but GO layers were completely separated at MGNO-120. These observations were confirmed by XRD and SEM analysis.
- TGA analysis results revealed that MGNO powders showed a superior thermal stability compared to GO.

Samples	DTG peak T (°C)				Weight loss at 600 °C (%)	Residue at 600 °C (%)
	T_{p1}	T_{p2}	T_{p3}	T_{p4}		
GO	78	185	269	558	86.7	13.3
MGNO-30	56	232	349		31.7	68.3
MGNO-120	65	209	288		60.7	39.3
MGNO-200	66	209	327		61.0	39.0
MGNO-300	53	209	351		46.6	53.4

Table 1: Thermal parameters for the GO and MGNO powders (20 °C × min^{-1} heating rate, under nitrogen atmosphere)

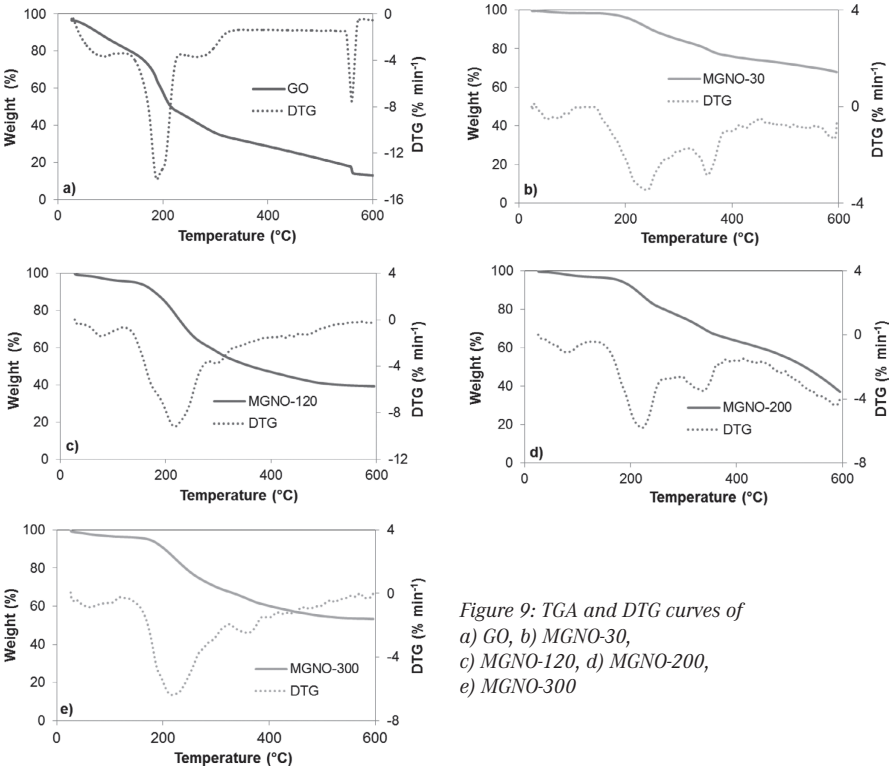

Figure 9: TGA and DTG curves of a) GO, b) MGNO-30, c) MGNO-120, d) MGNO-200, e) MGNO-300

References

1 X. Wang, L.-X. Gong, L.-C. Tang, K. Peng, Y.-B. Pei, L. Zhao, L.-B. Wu, J.-X. Jiang: Temperature dependence of creep and recovery behaviors of polymer composites filled with chemically reduced graphene oxide, Composites Part A 69 (2015), pp. 288-298 DOI:10.1016/j.compositesa.2014.11.031

2 I. Zaman, H.-C. Kuan, Q. Meng, A. Michelmore, N. Kawashima, T. Pitt, L. Zhang, S. Gouda, L. Luong, J. Ma: A facile approach to chemically modified graphene and its polymer nanocomposites, Advanced Functional Materials 22 (2012), No. 13, pp. 2735-2743 DOI:10.1002/adfm.201103041

3 K. Deshmukh, G. M. Joshi: Thermo-mechanical properties of poly(vinyl chloride)/graphene oxide as high performance nanocomposites, Polymer Testing 34 (2014), pp. 211-219 DOI:10.1016/j.polymertesting.2014.01.015

4 X. Yang, S. Shang, L. Li: Layer-structured poly(vinyl alcohol)/graphene oxide nanocomposites with improved thermal and mechanical properties, Journal of Applied Polymer Science 120 (2011), pp. 1355-1360 DOI:10.1002/app.33279

5 J. Li, D. Miao, R. Yang, L. Qu, P. B. Harrington: Synthesis of poly (sodium 4-styrenesulfonate) functionalized graphene/cetyltrimethylammonium bromide (CTAB) nanocomposite and its application in electrochemical oxidation of 2,4-dichlorophenol, Electrochimica Acta 125 (2014), pp. 1-8 DOI:10.1016/j.electacta.2014.01.068

6 T. Kuila, P. Khanra, A. K. Mishra, N. H. Kim, J. H. Lee: Functionalized-graphene/ethylene vinyl acetate co-polymer composites for improved mechanical and thermal properties, Polymer Testing 31 (2012), pp. 282-289 DOI:10.1016/j.polymertesting.2011.12.003

7 F. Kim, L. J. Cote, J. Huang: Graphene oxide: Surface activity and two-dimensional assembly, Advanced Materials 22 (2010), pp. 1954-1958 DOI:10.1002/adma.200903932

8 M. Veerapandian, M.-H. Lee, K. Krishnamoorthy, K. Yun: Synthesis, characterization and electrochemical properties of functionalized graphene oxide, Carbon 50 (2012), pp. 4228-4238 DOI:10.1016/j.carbon.2012.05.004

9 J. Hu, X. Jia, C. Li, Z. Ma, G. Zhang, W. Sheng, X. Zhang, Z. Wei: Effect of interfacial interaction between graphene oxide derivatives and poly(vinyl chloride) upon the mechanical properties of their nanocomposites, Journal of Material Science 49 (2014), pp. 2943-2951 DOI:10.1007/s10853-013-8006-1

10 S. Vadukumpully, J. Paul, N. Mahanta, S. Valiyaveettil: Flexible conductive graphene/poly(vinyl chloride) composite thin films with high mechanical strength and thermal stability, Carbon 49 (2011), pp. 198-205 DOI:10.1016/j.carbon.2010.09.004

11 S. Thakur, N. Karak: Green reduction of graphene oxide by aqueous phytoextracts, Carbon 50 (2012), pp. 5331-5339 DOI:10.1016/j.carbon.2012.07.023

12 X. Ji, L. Cui, Y. Xu, J. Liu: Non-covalent interactions for synthesis of new graphene based composites, Composites Science and Technology 106 (2015), pp. 25-31 DOI:10.1016/j.compscitech.2014.10.018

13 S. Shamaila, A. K. L. Sajjad, A. Iqbal: Modifications in development of graphene oxide synthetic routes, Chemical Engineering Journal 294 (2016), pp. 458-477 DOI:10.1016/j.cej.2016.02.109

14 Y. Wu, H. Luo, H. Wang, C. Wang, J. Zhang, Z. Zhang: Adsorption of hexavalent chromium from aqueous solutions by graphene modified with cetyltrimethylammonium bromide, Journal of Colloid and Interface Science 394 (2013), pp. 183-191 DOI:10.1016/j.jcis.2012.11.049

15 Y. Fan, Y. Liu, Q. Cai, Y. Liu, J. Zhang: Synthesis of CTAB-intercalated graphene/polypyrrole nanocomposites via in situ oxidative polymerization, Synthetic Metals162 (2012), pp. 1815-1821 DOI:10.1016/j.synthmet.2012.08.016

16 Y.-J. Wan, L.-C. Tang, D. Yan, L. Zhao, Y.-B. Li, L.-B. Wu, J.-X. Jiang, G.-Q. Lai: Improved dispersion and interface in the graphene/epoxy composites via a facile surfactant-assisted process, Composites Science and Technology 82 (2013), pp. 60-68 DOI:10.1016/j.compscitech.2013.04.009

17 H. Wang, X. Yuan, Y. Wu, H. Huang, X. Peng, G. Zeng, H. Zhong, J. Liang, M. Ren: Graphene-

based materials: fabrication, characterization and application for the decontamination of wastewater and waste gas and hydrogen storage/generation, Advances in Colloid and Interface Science195-196 (2013), pp. 19-40 DOI:10.1016/j.cis.2013.03.009
18 K. Brandt, C. Neusel, S. Behr, G. A. Schneider: Dielectric behaviour and conductivity of high-filled $BaTiO_3$–PMMA composites and the facile route of emulsion polymerization in synthesizing the same, Journal of Materials Chemistry C 1 (2013), pp. 3129-3137 DOI:10.1039/c3tc30204k
19 W. S. Hummers, R. E. Offeman: Preparation of graphitic oxide, Journal of the American Chemical Society 80 (1958), No. 6, pp. 1339-1339 DOI: 10.1021/ja01539a017
20 F. Mindivan: The synthesis and characterization of graphene oxide (GO) and reduced graphene oxide (RGO), Machines, Technologies, Materials 6 (2016), pp. 32-35
21 K. Krishnamoorthy, M. Veerapandian, K. Yun, S.-J. Kim: The chemical and structural analysis of graphene oxide with different degrees of oxidation, Carbon 53 (2013), pp. 38-49 DOI:10.1016/j.carbon.2012.10.013
22 B. White, S. Banerjee, S. O'Brien, N. J. Turro, I. P. Herman: Zeta-potential measurements of surfactant-wrapped Individual single-walled carbon nanotubes, The Journal of Physical Chemistry C 111 (2007), No. 37, pp. 13684-13690 DOI:10.1021/jp070853e
23 Z. Sun, V. Nicolosi, D. Rickard, S. D. Bergin, D. Aherne,J. N. Coleman: Quantitative evaluation of surfactant-stabilized single-walled carbon nanotubes: Dispersion quality and its correlation with zeta potential, The Journal of Physical Chemistry C 112 (2008), No. 29, pp. 10692-10699 DOI:10.1021/jp8021634
24 D. N. H. Tran, S. Kabiri, D. Losic: A green approach for the reduction of graphene oxide nanosheets using non-aromatic amino acids, Carbon 76 (2014), pp. 193-202 DOI:10.1016/j.carbon.2014.04.067
25 J. Song, X. Wang, C.-T. Chang: Preparation and characterization of graphene oxide, Journal of Nanomaterials 2014 (2014), pp. 1-6 DOI:10.1155/2014/276143
26 C. Bora, P. Bharali, S. Baglari, S. K. Dolui, B. K. Konwar: Strong and conductive reduced graphene oxide/polyester resin composite films with improved mechanical strength, thermal stability and its antibacterial activity, Composites Science and Technology 87 (2013), pp. 1-7 DOI:10.1016/j.compscitech.2013.07.025
27 Y. J. Yang, W. Li: CTAB functionalized graphene oxide/multi walled carbon nanotube composite modified electrode for the simultaneous determination of ascorbic acid, dopamine, uric acid and nitrite, Biosensors and Bioelectronics 56 (2014), pp. 300-306 DOI:10.1016/j.bios.2014.01.037
28 Y. Liu, Y. Zhang, G. Ma, Z. Wang, K. Liu, H. Liu: Ethylene glycol reduced graphene oxide/polypyrrole composite for supercapacitor, Electrochimica Acta 88 (2013), pp. 519-525 DOI:10.1016/j.electacta.2012.10.082
29 C.-C. Teng, C.-C. M. Ma, C.-H. Lu, S.-Y. Yang, S.-H. Lee, M.-C. Hsiao, M.-Y. Yen, K.-C. Chiou, T.-M. Lee: Thermal conductivity and structure of non-covalent functionalized graphene/epoxy composites, Carbon 49 (2011), pp. 5107-5116 DOI:10.1016/j.carbon.2011.06.095
30 N. Kumar, A. T. Kozakov, T. R. Ravindran, S. Dash, A. K. Tyagi: Load dependent friction coefficient of crystalline graphite and anomalous behavior of wear dimension, Tribology International 88 (2015), pp. 280-289 DOI:10.1016/j.triboint.2015.03.034
31 M. Safarpour, A. Khataee, V. Vatanpour: Thin film nanocomposite reverse osmosis membrane modified by reduced graphene oxide/TiO_2 with improved desalination performance, Journal of Membrane Science 489 (2015), pp. 43-54 DOI:10.1016/j.memsci.2015.04.010
32 D. Li, B. Zhang, F. Xuan: The sequestration of Sr(II) and Cs(I) from aqueous solutions by magnetic graphene oxides, Journal of Molecular Liquids 209 (2015), pp. 508-514 DOI:10.1016/j.molliq.2015.06.022
33 S. Stankovich, D. A. Dikin, R. D. Piner, K. A. Kohlhaas, A. Kleinhammes, Y. Jia, Y. Wu, S. T. Nguyen, R. S. Ruoff: Synthesis of graphene-based nanosheets via chemical reduction of exfoliated graphite oxide, Carbon 45 (2007), pp. 1558-1565 DOI:10.1016/j.carbon.2007.02.034
34 H. Liu, L. Hou, W. Peng, Q. Zhang, X. Zhang: Fabrication and characterization of polyamide 6-functionalized graphene nanocomposite fiber, Journal of Materials Science 47 (2012), pp. 8052-8060 DOI:10.1007/s10853-012-6695-5
35 Y. Jin, S. Huang, M. Zhang, M. Jia, D. Hu: A green and efficient method to produce graphene for electrochemical capacitors from graphene oxide using sodium carbonate as a reducing agent, Applied Surface Science 268 (2013), pp. 541-546 DOI:10.1016/j.apsusc.2013.01.004
36 R. F. Farias, C. Airoldi: Hexamethylenetetramine reaction with graphite oxide (GO) as a strategy to increase the thermal stability of GO: Synthesis and characterization of a compound, Journal of Serbian Chemical Society 75 (2010), No. 4, pp. 497-504 DOI:10.2298/JSC090717018D

Abstract

Auswirkung der verschiedenen CTAB-Anfangskonzentrationen auf die Struktur und thermische Stabilität von nicht-kovalentem modifizierten Graphenoxid (MGNO). Für die in diesem Beitrag beschriebene Studie wurde Graphenoxid (GO) durch Oxidationsreaktion von Graphit (GF) hergestellt, in dem das Hummers-Verfahren angewendet wurde, anschließend wurde dieses mit einem kationischen oberflächenaktiven Stoff (Cetyltrimethylammoniumbromid – CTAB) modifiziert, gefolgt von chemischer Reduktion mittels Hydrazin-Monohydrat ($N_2H_4 \times H_2O$), um MGNO-Pulver zu erhalten. Die strukturellen und die thermischen Eigenschaften der GO- und MGNO-Pulver wurde mittels Zeta Potentiometer (ZP), Fourier-Transformations-Infrarot-Spektroskopie (FTIR), Röntgendiffratometrie (XRD), Rasterelektronenmikroskopie (REM) und Thermogravimetrischer Analyse (TGA) untersucht. Die Ergebnisse zeigen, dass CTAB erfolgreich auf die Oberfläche des GO aufgebracht werden konnte, und zwar durch die nicht-kovalente Modifikation zwischen den CTA^+-Ionen und GO bei allen MGNO-Pulvern. Eine angemessene Verbesserung der thermischen Stabilität der MGNO-Pulver wurde ebenfalls beobachtet. Die FTIR-Ergebnisse zeigten die erfolgreiche Zwischeneinlagerung der CTA^+-Ionen bei allen MGNO-Pulvern. Die optimale Konzentration des oberflächenaktiven Stoffes wurde basierend auf den Analyseergebnissen mit 120 mg × l^{-1} (MGNO-120) ermittelt. Die Einfachheit der Synthese von MGNO-120 mit einer exzellenten Zwischeneinlagerung und thermischen Stabilität wird potentielle Anwendungen erheblich erleichtern.

Bibliography

DOI 10.3139/120.111063
Materials Testing
59 (2017) 9, pages 729-734

ISSN 0025-5300

The author of this contribution

Assistant Prof. Dr. Ferda Mindivan, born in 1983, graduated from Ataturk University, Erzurum, Turkey, Department of Chemistry, in 2005. After receiving her PhD degree from the same university in the field of Physical Chemistry in 2013, she is continuing her professional career as Assistant Professor in the Department of Technical programs at Bozuyuk Vocational College, Bilecik S. E. University, Bilecik, Turkey. Her main research interests include polymer matrix composites and their structural, thermal and mechanical characterization.